

Fabrication of cellulose aerogel from wheat straw with strong absorptive capacity

Jian LI (✉), Caichao WAN, Yun LU, Qingfeng SUN

Material Science and Engineering College, Northeast Forestry University, Harbin 150040, China

Abstract An effectively mild solvent solution containing NaOH/PEG was employed to dissolve the cellulose extracted from the wheat straw. With further combined regeneration process and freeze-drying, the cellulose aerogel was successfully obtained. Scanning electron microscope, X-ray diffraction technique, Fourier transform infrared spectroscopy, and Brunauer-Emmett-Teller were used to characterize this cellulose aerogel of low density (about $40 \text{ mg} \cdot \text{cm}^{-3}$) and three-dimensional network with large specific surface area (about $101 \text{ m}^2 \cdot \text{g}^{-1}$). Additionally, with a hydrophobic modification by trimethylchlorosilane, the cellulose aerogel showed a strong absorptive capacity for oil and dye solutions.

Keywords cellulose aerogel, absorptive capacity, waste wheat straw, freeze-drying

1 Introduction

Aerogel with a cross-linked three-dimensional network structure has attracted intensive attentions from academic communities and industrial fields, due to its low density [1–3], high specific surface area [4], high porosity [5], excellent thermal insulation [6] and extraordinary sound insulation ability [7]. It would be a great promising substance as adsorbing [8], heat barrier [9], acoustic insulation [10] or catalyst carrier [11]. The synthesis of aerogel could utilize a variety of raw materials such as silicon dioxide [12], metallic oxide [13] and some carbon-based materials [14], thus the aerogel derived from different categories of materials could acquire respective special property.

Cellulose, the most naturally renewable resource with

high mechanical performance [15], superior optical property [16] and active chemical reactivity, and has been regarded as a most promising substitution for the conventional materials. Among the newer cellulose-based materials, cellulose aerogel has received attention because of its high porosity, low density, fine flexibility and strong absorptive capacity. However, a suitable method to dissolve cellulose owing to its high crystallinity and polymerization (DP) as well as ultra-strong inter- and intra-molecular hydrogen bonds is pivotal for fabricating an environmentally sustainable aerogel [17,18]. Many effective cellulose solvents have been proposed such as ionic liquid [19–21], *N*-methylmorpholine-*N*-oxide (NMMO) [22], lithium chloride/*N,N*-dimethylacetamide (LiCl/DMAC) [23], NaOH/urea [24,25] and $\text{NH}_3/\text{NH}_4\text{SCN}$ [26]. Nevertheless, most of these are limited by their high cost, toxicity or volatility. Recently, mild and environmentally-friendly aqueous solution containing NaOH/PEG showed effective cellulose dissolution, which could contribute to the fabrication various cellulose-based products including cellulose aerogel.

Here we describe fabrication of a cellulose aerogel with superior adsorptive capacity from the wheat straw through dissolution, regeneration and freeze-drying. Furthermore, absorptive capacity of this product for oil and dye solutions was also investigated.

2 Materials and methods

2.1 Materials

Waste wheat straw was collected from the field and further completely cleaned, ground to a powder and passed through a 60-mesh sieve and dried at 60°C for 24 h. All chemical reagents were supplied by Shanghai Boyle chemical Co. Ltd.

Received March 6, 2014; accepted March 26, 2014

Correspondence: nefulijian@163.com

2.2 Extraction and purification of the cellulose from wheat straw

The processed wheat straw was first treated by a mixed solution of benzene/absolute ethanol (2:1 v/v) in a Soxhlet extractor at 90°C for 6 h. Then, the treated sample was air dried and treated with a 10% NaClO₂ solution (pH4.5 adjusted by glacial acetic acid) at 75°C for 5 h. The next step was to collect the sample by filtration and wash it three times with deionized water, and then immediately treat it with 2% NaOH at 90°C for 2 h. The product was again collected by filtration and washed three times with deionized water before treating it with 1% HCl at 80°C for 2 h. Finally, the purified cellulose was collected by filtration and washed three times deionized water and dried at 60°C for 24 h.

2.3 Preparation of cellulose aerogel

Sub-samples of the purified cellulose was added to an 10% aqueous solution of NaOH/PEG (9:1 wt/wt) with magnetic stirring for 5 h to form a homogeneous solution. This was repeated at mass ratios of 1/100, 2/100, 4/100 and 8/100 cellulose to the NaOH/PEG solution (referred to as C1, C2, C4 and C8, respectively, within this paper). These solutions were frozen for 12 h at -15°C then subsequently thawed at ambient temperature with vigorous stirring for 30 min. This process was repeated at least 3 times. The product was successively regenerated by 1 % HCl solution, distilled water and tertiary butanol until the formation of an amber-like hydrogel. Finally, the resultant cellulose hydrogel samples were freeze-dried at -30°C for 48 h.

2.4 Hydrophobic modification of the cellulose aerogel

The prepared cellulose aerogel was modified using trimethylchlorosilane (TMCS) through a chemical vapor deposition method. TCMS (300 L) was dispensed into a 5 mL beaker and placed in a desiccator. Afterwards, the cellulose aerogel samples were also put into the desiccator avoiding direct contact with the TMCS. Within the desiccator, the sample and TMCS allowed to react for 24 h at ambient temperature. This process successfully fabricated hydrophobic aerogel.

2.5 Cellulose aerogel characterization

Sample morphology was examined by a scanning electron microscope (SEM, Quanta 200, FEI). Crystalline structures were identified by X-ray diffraction technique (Rigaku, D/MAX 2200) operating with Cu K α radiation ($\lambda = 1.5418 \text{ \AA}$) at a scan rate (2θ) of $4^\circ \cdot \text{min}^{-1}$, 40 kV, 40 mA ranging from 5° to 40° . Chemical compositions were recorded by Fourier transform infrared spectroscopy (Magna-IR 560, Nicolet). Specific surface area and pore

size distribution of samples were characterized by Brunauer-Emmett-Teller analysis via an accelerated surface area and porosimetry system (3H-2000PS2 unit, Beishide Instrument S & T Co. Ltd.). Water contact angle (WCA) was measured on an OCA40 contact angle system (Dataphysics, Germany) at room temperature. The final value of the WCA was obtained as a mean of five measurements.

3 Results and discussion

Figure 1 shows stages in the fabrication of the cellulose aerogels made from wheat straw. In Fig. 1a, the purified cellulose was white with light yellow. When dissolved in the NaOH/PEG solution and regenerated by HCl solution, the cellulose turned into a transparent solution and then formed a solid white column (Fig. 1b and 1c), indicating the information of cellulose hydrogel via the regeneration process. During this process, the hydrogen bonds between the cellulose molecules and the solvent molecules of NaClO₂ and PEG were significantly damaged by the coagulator of HCl solution. The intra- and inter-molecular hydrogen bonds between the cellulose chains were reshaped and lead to the transformation of the hydrogel [3]. In Fig. 1d, the multiporous and light cellulose aerogel was formed after the freeze-drying. The bulk densities of C1, C2, C3 and C4 were 44.9, 56.7, 80.7 and $148.0 \text{ mg} \cdot \text{cm}^{-3}$, respectively. The bulk densities of the samples increased with the enhanced cellulose concentrations.

Figure 2 shows SEM images of the prepared cellulose aerogels with different concentrations. Though with obvious wide porous structures, there were still some significant differences for each sample. Apparently, the pore configurations of C1 and C2 in Fig. 2a and 2b were dense, anfractuous and multi-layered. In Fig. 2c and 2d, the pore distributions of C3 and C4 were relatively uniform. Some larger sheet and blocky regions surrounding with pore structures were observed. This might be attributed to the existence of undissolved fractional cellulose at high concentrations. It is concluded that the concentration had a significant influence on the pore structures of the aerogels.

Figure 3 presents the N₂ adsorption-desorption isotherms of C1, C2, C3 and C4, respectively. All the curves have inverse-S shape, which is type II adsorption curve according to IU-PAC classification [21]. Additionally, the hysteresis loop in the range of about 0.4–1.0 belongs to H3 type.

Furthermore, the pore diameter distributions of C1, C2, C3 and C4 were evaluated and are shown in Fig. 4. The pore sizes of all the samples are within the range 1 to 60 nm, and mainly consisted of micropores (< 2 nm) and mesopores (2–50 nm). Most pores were at the central range of 1 to 10 nm.

The detailed specific surface area and pore diameter



Fig. 1 Steps in the preparation of cellulose aerogel. (a) Purified cellulose from waste wheat straw; (b) cellulose solution; (c) cellulose hydrogel; (d) cellulose aerogel.

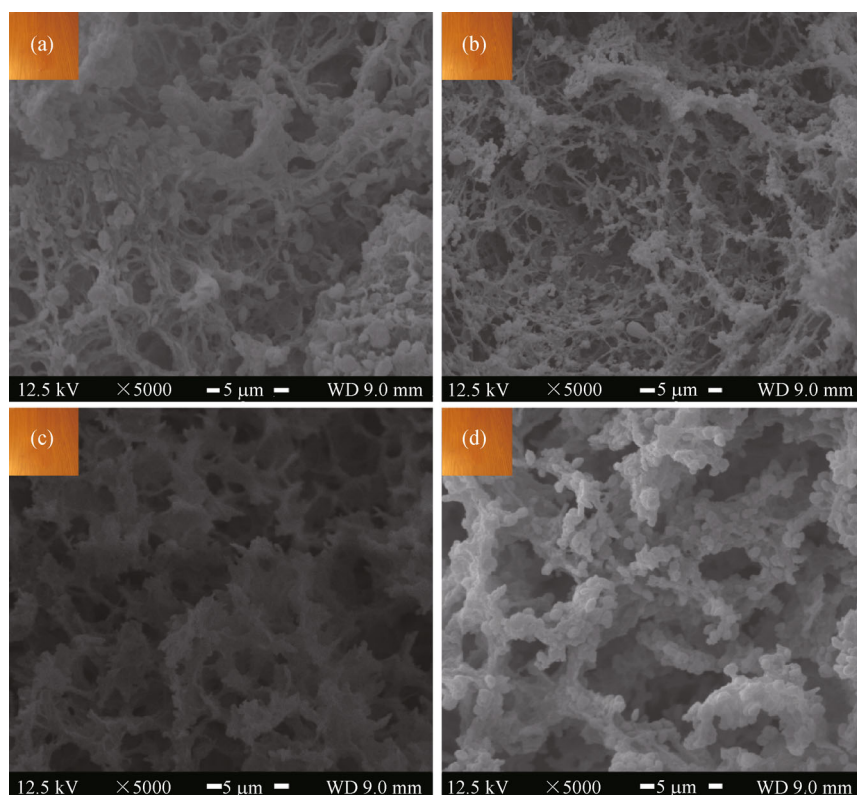


Fig. 2 SEM images of cellulose aerogel samples fabricated with mass ratios of 1/100 (a), 2/100 (b), 4/100 (c) and 8/100 (d) cellulose to the NaOH/PEG solution

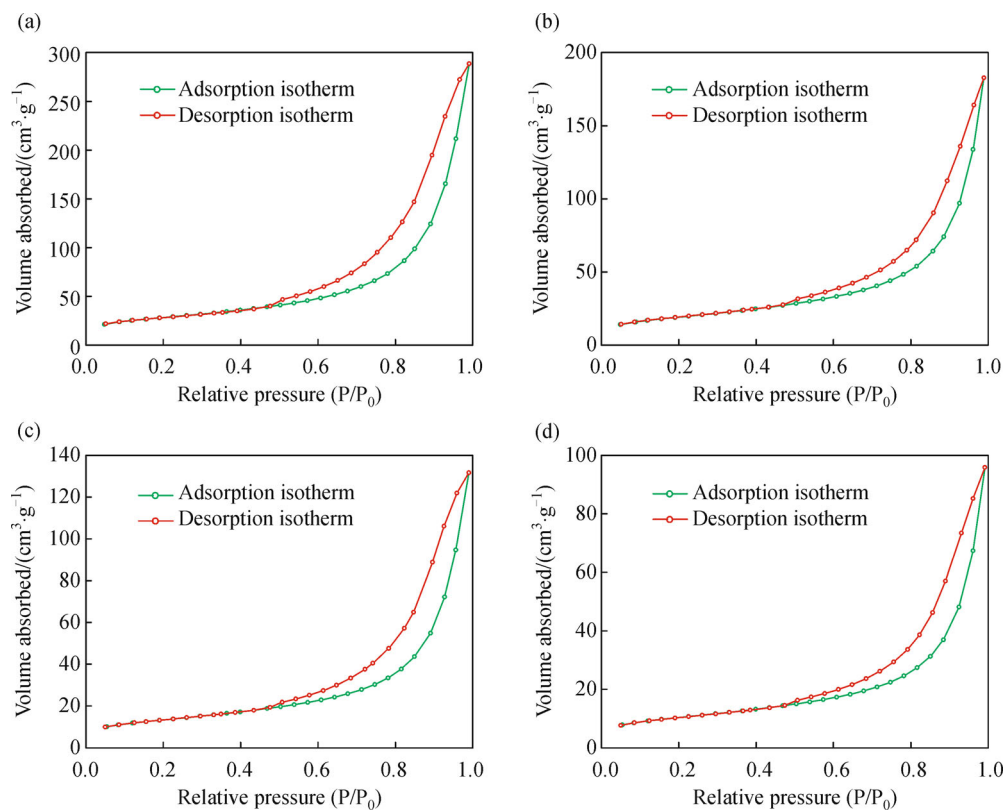


Fig. 3 N_2 adsorption-desorption isotherms of cellulose aerogel samples fabricated with mass ratios of 1/100 (a), 2/100 (b), 4/100 (c) and 8/100 (d) cellulose to the NaOH/PEG solution

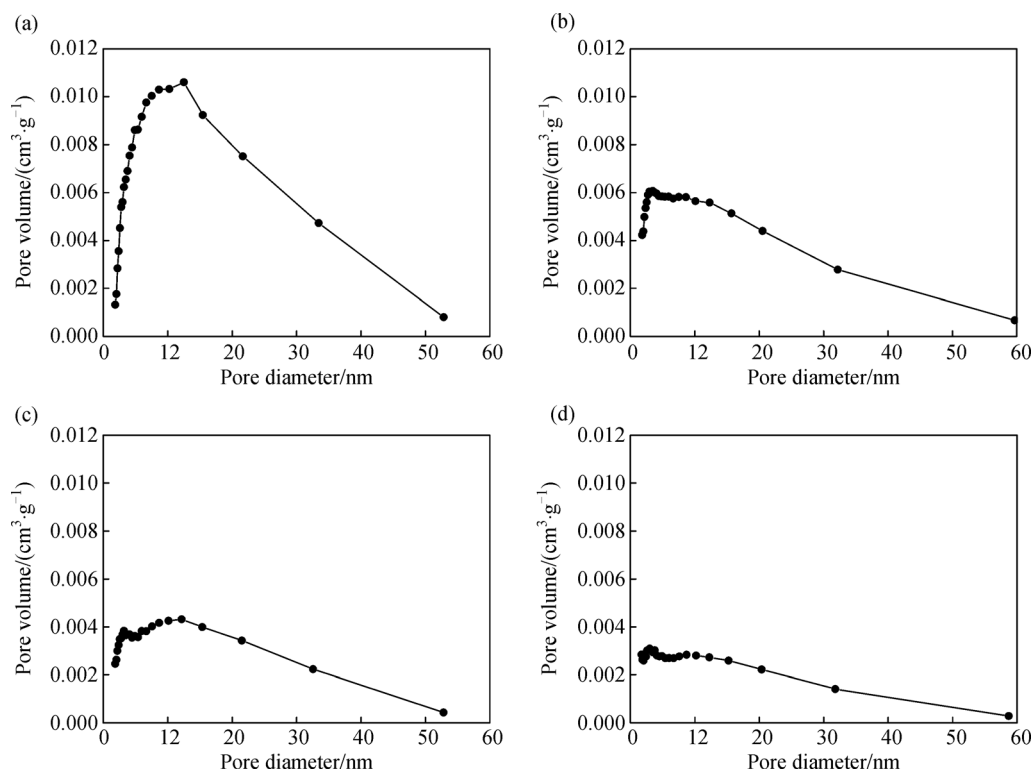


Fig. 4 Pore diameter distributions of cellulose aerogel samples fabricated with mass ratios of 1/100 (a), 2/100 (b), 4/100 (c) and 8/100 (d) cellulose to the NaOH/PEG solution

distribution are shown in Table 1. Apparently, there were negative correlations between specific surface area, mean pore diameter and total pore volume, and the cellulose solution concentration. Furthermore, the large specific surface area, mean pore diameter and pore volume might be able to adsorb considerable amounts of gases or liquids.

Figure 5 shows X-ray diffraction patterns and Fourier transform infrared spectroscopy spectra of the wheat straw, purified cellulose and cellulose aerogel (C1, C2, C4 and C8). As evident in Fig. 5a, the wheat straw and the purified cellulose samples were typical cellulose I structure due to the crystalline peaks at 15.8° and 22.2° [27]. However, for C1, C2, C4 and C8, the crystalline peaks were shifted to lower peaks at 12.1° , 20.0° and 22.0° , respectively. It appears that the crystalline structure of the cellulose transformed from cellulose I to cellulose II. The crystallinity calculated by Segal's method [28] of the raw material, cellulose, C1, C2, C4 and C8 were 53.7%, 67.6%, 70.1%, 69.6%, 69.1%, 68.8% and 69.1%, respectively. It was observed that the cellulose aerogels preparations had a higher crystallinity than that of the raw material, presumably due to the removal of hemicellulose and lignin when purified.

In Fig. 5b, the peaks at 3320 and 2883 cm^{-1} attributed to $-\text{OH}$ and $-\text{CH}$ stretching vibrations were observed in the complete spectra for each sample. After the purified process, the peak recorded for wheat straw at 1739 cm^{-1}

attributed either to the acetyl groups of the hemicellulose carboxylic groups in lignin and/or hemicellulose almost disappeared. This indicates that most of the hemicellulose and lignin were removed from the wheat straw through the chemical purification. A peak at 1631 cm^{-1} contributed to the $\text{H}-\text{O}-\text{H}$ stretching vibration of absorbed water was still observed in all the samples with a slight decrease in intensity, which indicates that a small amount of hemicellulose still exist in the purified cellulose and the fabricated cellulose aerogel. Compared with the purified cellulose, the peak at 1434 cm^{-1} attributed to $-\text{CH}_2$ shifted to lower value (1432 cm^{-1}) observed for the aerogels implying the crystalline transformation of the cellulose from I to II [29].

Figure 6a shows water drops standing on the surface of the modified aerogel by TMCS. For untreated cellulose aerogel, the water drops were immediately absorbed due to its inherent hydrophilicity and abundant pore structure. Whereas, the water drops could stay on the modified aerogel surface with a WCA of 138° (Fig. 6a insert). In Fig. 6b, aerogel immersion into the water further confirmed its hydrophobicity. The extraordinary hydrophobic performance of the treated cellulose aerogel could be used to facilitate for the separation of oil-water.

Figure 7 shows the absorptive capacity of the cellulose aerogel for oil and dye solutions. Oil, rhodamine B, methyl orange and indigo blue were efficiently absorbed by the

Table 1 Specific surface area, mean pore diameter, total pore volume and nanoparticle size of cellulose aerogel samples fabricated with mass ratios of 1/100, 2/100, 4/100 and 8/100 cellulose to the NaOH/PEG solution (C1, C2, C3 and C4, respectively)

	Specific surface area $/(\text{m}^2 \cdot \text{g}^{-1})$	Mean pore diameter $/\text{nm}$	Total pore volume $/(\text{cm}^3 \cdot \text{g}^{-1})$	Nanoparticle size $/\text{nm}$
C1	101.13	18.32	0.47	60.50
C2	68.34	16.54	0.28	87.80
C4	47.34	17.21	0.20	126.75
C8	36.46	16.27	0.15	164.57

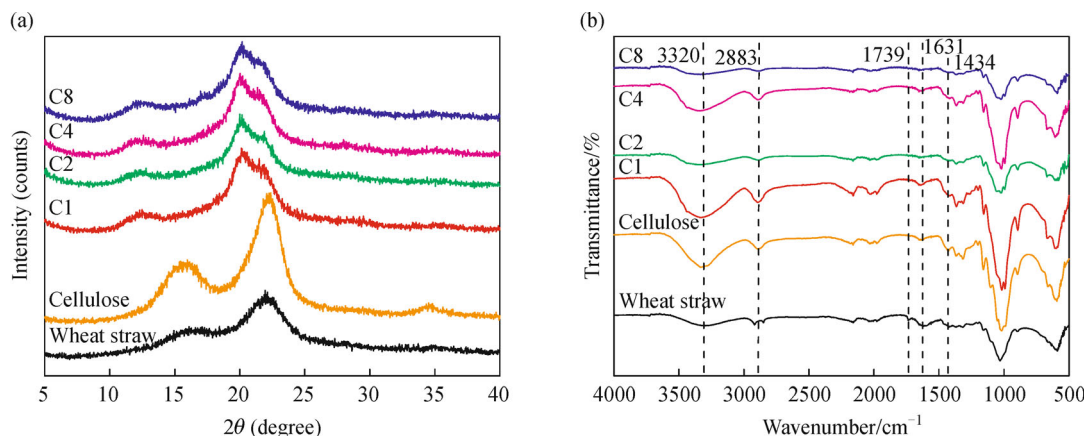


Fig. 5 X-ray diffraction patterns (a) and Fourier transform infrared spectra (b) of the wheat straw, the purified cellulose, and cellulose aerogel samples (fabricated with mass ratios of 1/100, 2/100, 4/100 and 8/100 cellulose to the NaOH/PEG solution, C1, C2, C4 and C8, respectively)

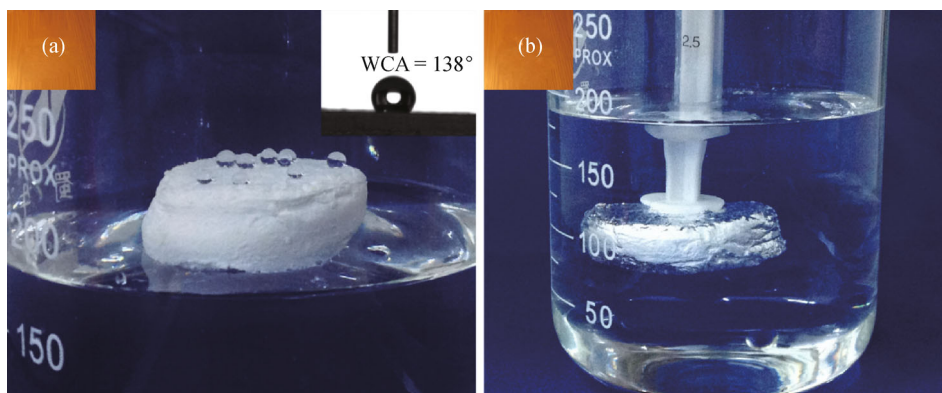


Fig. 6 Water drops standing on the TMCS treated cellulose aerogel and water contact angle (insert) (a) and modified cellulose aerogel immersed into the water under external pressure (b)

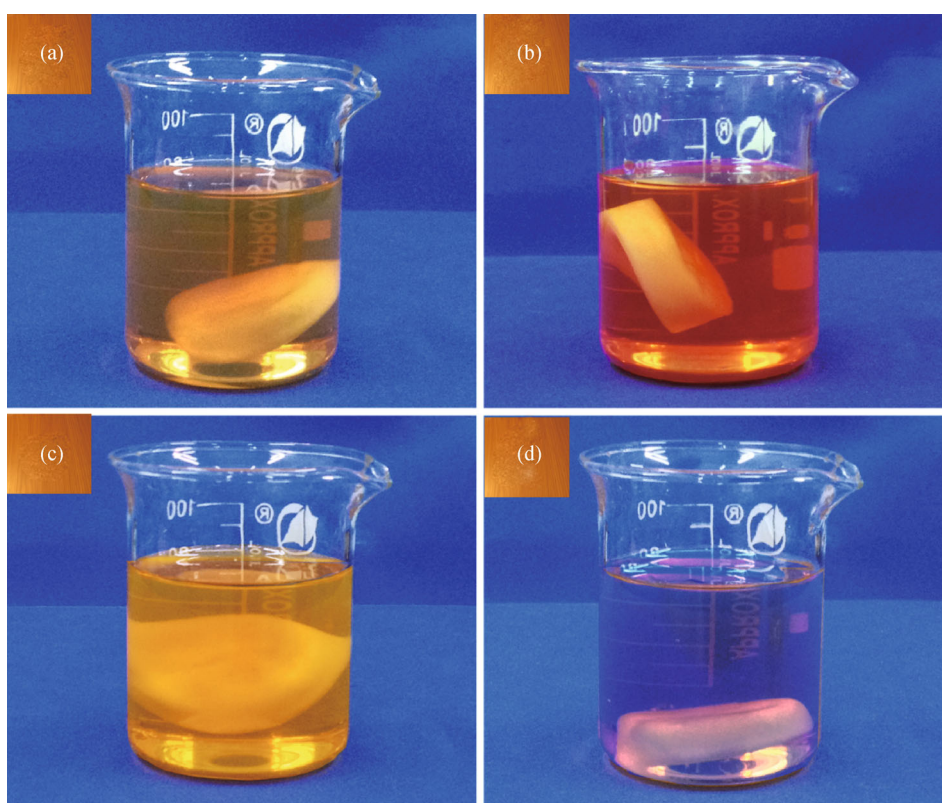


Fig. 7 Absorbed performance of the hydrophobic cellulose aerogels in motor oil (a), Rhodamine B solution (b), methyl orange solution (c), and indigo blue solution (d)

cellulose aerogel with respective absorptive capacities of about 18.7, 17.3, 16.8 and 17.4 times by weight. Consequently, the cellulose aerogel preparations could potentially be widely used for separating wastewater or oil spills.

4 Conclusions

Cellulose aerogel was successfully fabricated from wheat

straw by an environmentally-friendly NaOH/PEG solvent system. The cellulose aerogel revealed a dense and interconnected three-dimensional network structure. In addition, the hydrophobic modified cellulose aerogel showed a strong and superior absorption capacity for oil and dye solutions.

Acknowledgements This work was financially supported by the National Natural Science Foundation of China (31270590), China Postdoctoral

Science Foundation funded project (2013M540263) and Doctoral Candidate Innovation Research Support Program of Science & Technology Review (kjdb2012006).

Compliance with ethics guidelines Jian Li, Caichao Wan, Yun Lu and Qingfeng Sun declare that they have no conflict of interest or financial conflicts to disclose.

This article does not contain any studies with human or animal subjects performed by the any of the authors.

References

- Baetens R, Jelle B P, Gustavsen A. Aerogel insulation for building applications: a state-of-the-art review. *Energy and Building*, 2011, 43(4): 761–769
- Jones S M. Aerogel: space exploration applications. *Journal of Sol-Gel Science and Technology*, 2006, 40(2–3): 351–357
- Pierre A C, Pajonk G M. Chemistry of aerogels and their applications. *Chemical Reviews*, 2002, 102(11): 4243–4266
- Liu N, Shen J, Liu D. Activated high specific surface area carbon aerogels for EDLCs. *Microporous and Mesoporous Materials*, 2013, 167: 176–181
- Takeuchi H, Higashitani S, Nagai K, Choi H C, Moon B H, Masuhara N, Meisel M W, Lee Y, Mulders N. Knudsen-to-hydrodynamic crossover in liquid ^3He in a high-porosity aerogel. *Physical Review Letters*, 2012, 108(22): 225307
- Smith D M, Maskara A, Boes U. Aerogel-based thermal insulation. *Journal of Non-Crystalline Solids*, 1998, 225: 254–259
- Akimov Y K. Fields of application of aerogels. *Instruments and Experimental Techniques*, 2003, 46(3): 287–299
- Bag S, Trikalitis P N, Chupas P J, Armatas G S, Kanatzidis M G. Porous semiconducting gels and aerogels from chalcogenide clusters. *Science*, 2007, 317(5837): 490–493
- Li S, Wang C A, Hu L. Improved heat insulation and mechanical properties of highly porous YSZ ceramics after silica aerogels impregnation. *Journal of the American Ceramic Society*, 2013, 96(10): 3223–3227
- Hrubesh L W, Poco J F. Thin aerogel films for optical, thermal, acoustic and electronic applications. *Journal of Non-Crystalline Solids*, 1995, 188(1–2): 46–53
- Bang Y, Han S J, Yoo J, Park S, Choi J H, Lee Y J, Song J H, Song I K. Hydrogen production by steam reforming of liquefied natural gas (LNG) over mesoporous nickel–phosphorus–alumina aerogel catalyst. *International Journal of Hydrogen Energy*, 2014, 39(10): 4909–4916
- Henning S, Svensson L. Production of silica aerogel. *Physica Scripta*, 1981, 23(4B): 697–702
- Davis M, Ramirez D A, Hope-Weeks L J. Formation of three-dimensional ordered hierarchically porous metal oxides via a hybridized epoxide assisted/colloidal crystal templating approach. *ACS Applied Materials & Interfaces*, 2013, 5(16): 7786–7792
- Zhang L L, Zhao X S. Carbon-based materials as supercapacitor electrodes. *Chemical Society Reviews*, 2009, 38(9): 2520–2531
- Nakagaito A, Yano H. The effect of morphological changes from pulp fiber towards nano-scale fibrillated cellulose on the mechanical properties of high-strength plant fiber based composites. *Applied Physics A-Materials Science & Processing*, 2004, 78(4): 547–552
- Lavoine N, Desloges I, Dufresne A, Bras J. Microfibrillated cellulose—its barrier properties and applications in cellulosic materials: a review. *Carbohydrate Polymers*, 2012, 90(2): 735–764
- Wu J, Zhang J, Zhang H, He J, Ren Q, Guo M. Homogeneous acetylation of cellulose in a new ionic liquid. *Biomacromolecules*, 2004, 5(2): 266–268
- Zhang H, Wu J, Zhang J, He J. 1-Allyl-3-methylimidazolium chloride room temperature ionic liquid: a new and powerful nonderivatizing solvent for cellulose. *Macromolecules*, 2005, 38(20): 8272–8277
- Zhu S, Wu Y, Chen Q, Yu Z, Wang C, Jin S, Ding Y, Wu G. Dissolution of cellulose with ionic liquids and its application: a mini-review. *Green Chemistry*, 2006, 8(4): 325–327
- Lu Y, Sun Q, Yang D, She X, Yao X, Zhu G, Liu Y, Zhao H, Li J. Fabrication of mesoporous lignocellulose aerogels from wood via cyclic liquid nitrogen freezing–thawing in ionic liquid solution. *Journal of Materials Chemistry*, 2012, 22(27): 13548–13557
- Li J, Lu Y, Yang D, Sun Q, Liu Y, Zhao H. Lignocellulose aerogel from wood-ionic liquid solution (1-allyl-3-methylimidazolium chloride) under freezing and thawing conditions. *Biomacromolecules*, 2011, 12(5): 1860–1867
- Fink H P, Weigel P, Purz H, Ganster J. Structure formation of regenerated cellulose materials from NMMO-solutions. *Progress in Polymer Science*, 2001, 26(9): 1473–1524
- Tosh B, Saikia C N, Dass N N. Homogeneous esterification of cellulose in the lithium chloride–N,N-dimethylacetamide solvent system: effect of temperature and catalyst. *Carbohydrate Research*, 2000, 327(3): 345–352
- Cai J, Liu S, Feng J, Kimura S, Wada M, Kuga S, Zhang L. Cellulose-silica nanocomposite aerogels by *in situ* formation of silica in cellulose gel. *Angewandte Chemie International Edition*, 2012, 51(9): 2076–2079
- He M, Zhao Y, Duan J, Wang Z, Chen Y, Zhang L. Fast contact of solid-liquid interface created high strength multi-layered cellulose hydrogels with controllable size. *ACS Applied Materials & Interfaces*, 2014, 6(3): 1872–1878
- Cuculo J A, Smith C B, Sangwatanaroj U, Stejskal E O, Sankar S S. A study on the mechanism of dissolution of the cellulose/ NH_3 / NH_4SCN system. I. *Journal of Polymer Science Part A: Polymer Chemistry*, 1994, 32(2): 229–239
- Han D, Yan L. Preparation of all-cellulose composite by selective dissolving of cellulose surface in PEG/NaOH aqueous solution. *Carbohydrate Polymers*, 2010, 79(3): 614–619
- Segal L, Creely J, Martin A, Conrad C. An empirical method for estimating the degree of crystallinity of native cellulose using the X-ray diffractometer. *Textile Research Journal*, 1959, 29(10): 786–794
- French A D, Santiago Cintrón M. Cellulose polymorphism, crystallite size, and the Segal crystallinity index. *Cellulose*, 2013, 20(1): 583–588